Progress In Electromagnetics Research C, Vol. 73, 87–95, 2017

Inkjet Printing of a 20 GHz Coplanar Waveguide Monopole Antenna Using Copper Oxide Nanoparticles on Flexible Substrates: Effect of Drop Spacing on Antenna Performance

Shaimaa A. Mohassieb[1, 2], Khaled Kirah[2], Edgar Dörsam[3], Ahmed S. G. Khalil[4, 5, *], and Hadia M. El-Hennawy[2]

Abstract—Coplanar monopole antennas printed using copper oxide nanoparticles on flexible substrates are characterized in order to study the effect of the ink drop spacing on the antenna parameters. Polyethylene Terephthalate and Epson paper were the chosen flexible substrates, and the antennas were designed to operate at 20 GHz. A maximum conductivity of $2.8 \times 10^7\,\Omega^{-1}\mathrm{m}^{-1}$ was obtained for the films printed on Polyethylene Terephthalate using a drop spacing of 20 µm. The corresponding antenna achieved a gain and an efficiency of 1.82 dB and 97.6%, respectively. Experiments showed that smaller drop spacings lead to bulging of the printed lines while the antenna performance worsens for longer ones. At the same drop spacing, antennas printed on Epson paper substrate showed a −10 dB return loss bandwidth which extended from 17.9 GHz to 23.3 GHz, leading to a fractional bandwidth of 26.0%.

1. INTRODUCTION

Printed electronic technology has expanded due to its ability to substantially lower the production costs of a variety of active electronic devices and to the possibility of fabricating new ones. Flexible displays, low-cost circuits such as radio-frequency identification tags (RFID) [1] and different types of embedded sensors [2] are just examples. By printing only the required devices and connections, the costly multistep procedure of photolithography is replaced by the much simpler and lower cost steps of addition and sintering of a material to a substrate. Printing is also suitable for a variety of low-cost non-traditional flexible substrates such as paper, textiles, metal foils and polymers [3–5]. Several printing technologies including gravure printing [6–8], screen printing [9, 10], and inkjet printing [11–14] were used to deposit conducting, semiconducting and insulating films. While gravure printing is used when high throughput and high resolution are required, screen printing is best for low resolution thick films. Gravure printing is thus suitable to produce low cost circuits like RFID chips while screen printing is more towards applications like large resistance wires. On the other hand, inkjet printing is appropriate for applications requiring medium to high printing resolutions and a wide range of throughputs. In order to bring further advances, the printing parameters such as drop spacing (DS), drop diameter and the spacing between adjacent lines must be optimized.

In this paper, coplanar waveguide (CPW) feed monopole antennas printed on the flexible substrates Polyethylene Terephthalate (PET) and on Epson paper were designed for operating at 20 GHz. Copper oxide based ink with drop spacings from 15 µm to 35 µm was investigated for each substrate in order to find the optimum value. Evaluation of the antenna parameters for all cases was done taking into considerations the conductivity of the printed films. Experimental results showed very good agreement with simulation ones.

Received 8 February 2017, Accepted 25 March 2017, Scheduled 11 April 2017

* Corresponding author: Ahmed Saad G. Khalil (ahmed.s.g.khalil@uni-due.de).

[1] Akhbar Elyom Academy, 6th October City, Egypt. [2] Faculty of Engineering, Ain Shams University, Cairo, Egypt. [3] Institute of Printing Science and Technology, Technical University of Darmstadt, Darmstadt, Germany. [4] Arab Academy for Science, Technology and Maritime Transport, Smart Village Campus, Giza, Egypt. [5] Center for Environmental and Smart Technology, Faculty of Science, Fayoum University, Fayoum, Egypt.

2. EXPERIMENTAL

2.1. Printing Conditions

Antenna implementation was done with the inkjet printing technology (IJPT). A Fujifilm inkjet Dimatix Materials printer DMP-2800 (Fujifilm Dimatix, Inc. Santa Clara, USA) was used [15]. It requires an ink of intermediate viscosity. The ink used is Novacentrix Metalon® ICI-002HV Nanocopper oxide Ink-Aqueous dispersion, CuO content 16 wt% (CuONP). Cu has the second highest electrical conductivity among metals (bulk value is $5.96 \times 10^7\,\Omega^{-1}\mathrm{m}^{-1}$ compared to $6.3 \times 10^7\,\Omega^{-1}\mathrm{m}^{-1}$ for silver).

Novacentrix Novele^{TM}IJ-220 Polyethylene Terephthalate and Epson paper were used as dielectric substrates. PET and paper differ on how the ink interacts with their surface. In the case of the porous Epson paper, the ink spread on its surface, dries instantaneously and is slightly maroon. On the other hand and for the non-porous PET, the ink remains wet and becomes dark-brown after sintering. Trials have shown that ink droplet diameters of 38 µm and 40 µm for PET and for paper respectively are appropriate. These chosen values are highly dependent on the characteristics and interaction of the fluid being jetted and the substrate. The printer conditions for both substrates are not the same due to the thickness difference of the films on each type of substrate. The adjusted printing parameters are illustrated in Table 1.

Table 1. Printer conditions for PET and paper substrates.

Specifications	PET	Paper
Firing voltage (V)	29.7	29.0
Meniscus set point	5.0	1.0
Cartridge height (mm)	0.5	0.7
Platen height (mm)	0.14	1.0
Platen Temperature	30°C	30°C

For each substrate and in order to optimize the printing process, drop spacings from 15 µm to 35 µm were tested. As expected, too close drops cause the formation of bulges along the length of the line while large DSs result in scalloped patterns [16, 17] as it will be detailed in the next section.

2.2. Photo Sintering

A curing process is performed immediately after printing in order to transform the copper oxide-based ink into a metallic copper thin film. A Novacentrix PulseForge 1200 photonic curing system was used for this purpose. Photonic sintering is based on the distinctly higher absorption of metal nanoparticles to visible light compared to paper and polymeric films [18]. Samples are dried fast enough due to the high-energetic intense-pulsed light (IPL) sintering to form a flat copper layer without being blown off. Good percolation channels for electrons to flow are created when the curing temperature and time are adjusted. Besides that, nanoscale cracks are reduced and bonding to the substrate is increased [19]. It was found that the curing conditions for both PET and Epson paper substrate are the same. Trials showed that optimum drying conditions are satisfied by a two consecutive steps. The first one was done at a voltage of 330 V with 11 micro pulses of 0.3 duty cycle and total length 7.5 ms. In the second step, a voltage of 410 V, 11 micro pulses of 0.3 duty cycle and total length 5 ms were used. It was also found that if the voltage and pulse duration exceed these values, CuNP layer will flack off due to adhesion and absorption characteristics for both substrates. Fig. 1(a) shows line morphologies for different DSs after photonic sintering with values 35 µm, 30 µm, 20 µm and 15 µm starting from the left respectively while Fig. 1(b) shows a scanning electron microscope (SEM) picture for the printed CuNP line on PET at drop spacing of 20 µm. For DSs of 35 µm and more, the copper nanoparticles are separated from each others and therefore act as open circuit. Figs. 1(c) and 1(d) show the formation of agglomeration and bulges in printed lines at drop spacing 15 µm after photo sintering for CuONP ink on PET and on Paper respectively. Therefore, films printed from drop spacings with the values 20, 25 and 30 µm only were used to fabricate the antennas.

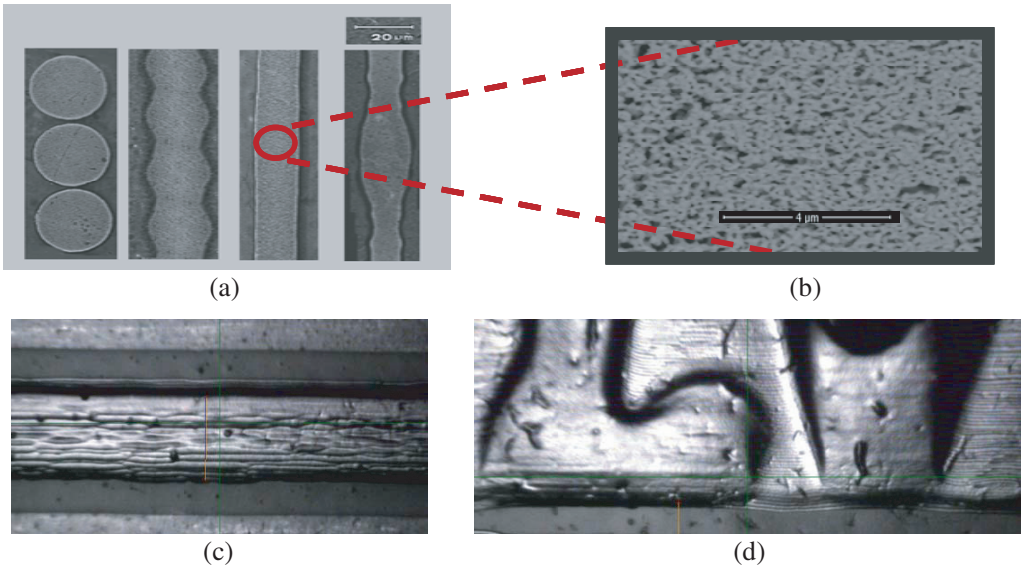

Figure 1. (a) Printed lines morphologies after photonic curing with the DS decreasing from left (35 µm) to right (15 µm). (b) SEM picture of a printed line on PET substrate at DS 20 µm. (c) The formation of agglomeration and bulges in printed lines at drop spacing 15 µm after photo sintering for CuONP ink on PET and (d) on paper.

2.3. Antenna Design and Printing

A CPW antenna is formed from a central strip of width S and separated by two narrow slits of width g from two ground planes of width w_g as shown in Fig. 2. This symmetric structure has the patch and feed line on the same side of the substrate. This eliminates the alignment problem needed in other wideband feeding techniques such as aperture coupled and proximity feed. The antenna is designed for an operating frequency of 20 GHz. The 3D full-wave EM simulation software CST Microwave Studio 2015 is used to calculate the optimum antenna dimensions for both substrates. The optimized dimensions are illustrated in Table 2. The antenna designs as well as all the printing setup conditions are then uploaded to the printer using the accompanying software.

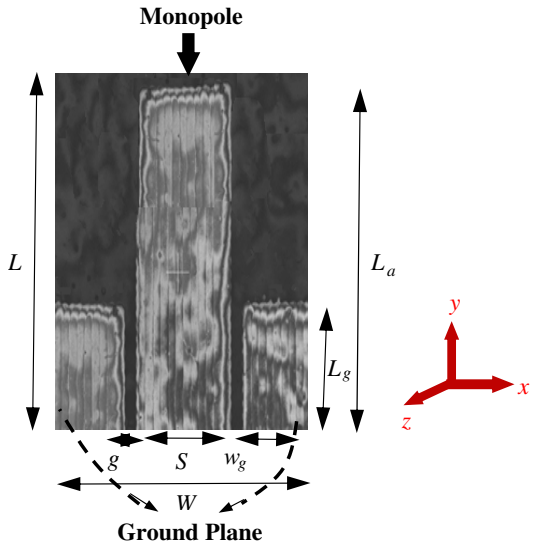

Figure 2. Micrograph of the fabricated CPW monopole antenna showing the dimensions calculated in Table 2.

Table 2. Optimized antenna dimensions for PET and paper substrates.

	Specifications	Ink droplet (μm)	DS (μm)	L (mm)	W (mm)	S (mm)
PET	Relative permittivity: 3.4 Dielectric height: 140 μm CuONP thickness refer to Fig. 3(b)	38	20	6.61	5.946	0.378
			25	6.608	5.896	0.363
			30	6.583	5.886	0.338
Paper	Relative permittivity: 4.2 Dielectric height: 700 μm CuNP thickness refer to Fig. 3(b)	40	20	5.475	5.94	0.88
			25	5.46	5.93	0.866
			30	5.455	5.92	0.85
	Specifications	g (mm)	La (mm)	Lg (mm)	Wg (mm)	-
PET	Relative permittivity: 3.4 Dielectric height: 140 μm CuONP thickness refer to Fig. 3(b)	0.046	3.965	0.995	2.738	-
		0.053	3.963	0.988	2.713	-
		0.066	3.938	0.966	2.708	-
Paper	Relative permittivity: 4.2 Dielectric height: 700 μm CuONP thickness refer to Fig. 3(b)	0.11	4.08	1.78	2.42	-
		0.117	4.065	1.765	2.415	-
		0.125	4.06	1.75	2.41	-

The table also shows that by increasing the drop spacing, the strip width S decreases while the gap g increases for both dielectric substrates. Also, the antenna length L_a and width W decrease when the drop spacing increases.

3. RESULTS AND DISCUSSION

3.1. Drop Spacing Effect

Drop spacing is an important parameter which must be optimized in order to obtain smooth and straight printed lines. Along with the drop diameter, the DS are determined according to the viscosity of the used ink and the angle of contact with the substrate [20]. As explained in Section 2.1, only drop spacings with values 20 μm, 25 μm and 30 μm were used to fabricate the antennas on both substrates. The sheet resistance was measured by the Van-der-Pauw method [21]. The thin film thickness was determined by a Sensofar PLuNeox profilometer and the line width was found by a Fludicial camera [22, 23]. The obtained results of these parameters for each drop spacing are shown in Fig. 3.

Figure 3(a) shows that the electrical sheet resistance increases with the increase of the DSs. On the other hand, Figs. 3(b) and 3(c) reveal that increasing the drop spacing decreases the film thickness and the strip width for both substrates. The calculated conductivity in Fig. 3(d) is higher for the PET case and decreases for both substrates as the DS increases.

This clearly shows that the smaller the DSs are, the more homogeneous the printed lines are. Smaller drop spacings lead to an overlap which form better paths for the current. A maximum conductivity of about $2.8 \times 10^7\,\Omega^{-1}\mathrm{m}^{-1}$ was achieved in the case of PET with DS = 20 μm. This is about 47% of the bulk material value and is well within the best published results [24, 25]. Better conductivity is found for PET since the surface energy of the substrate is greater than the surface tension of the ink [26]. This causes ink drops to be better spread on the non-porous substrate contrary to the paper substrate.

3.2. Antenna Parametric Study

The simulated reflection coefficients for each substrate at different drop spacing are shown in Fig. 4. The best reflection coefficient $|S_{11}|$ is obtained at drop spacing 20 μm for both substrates with a better

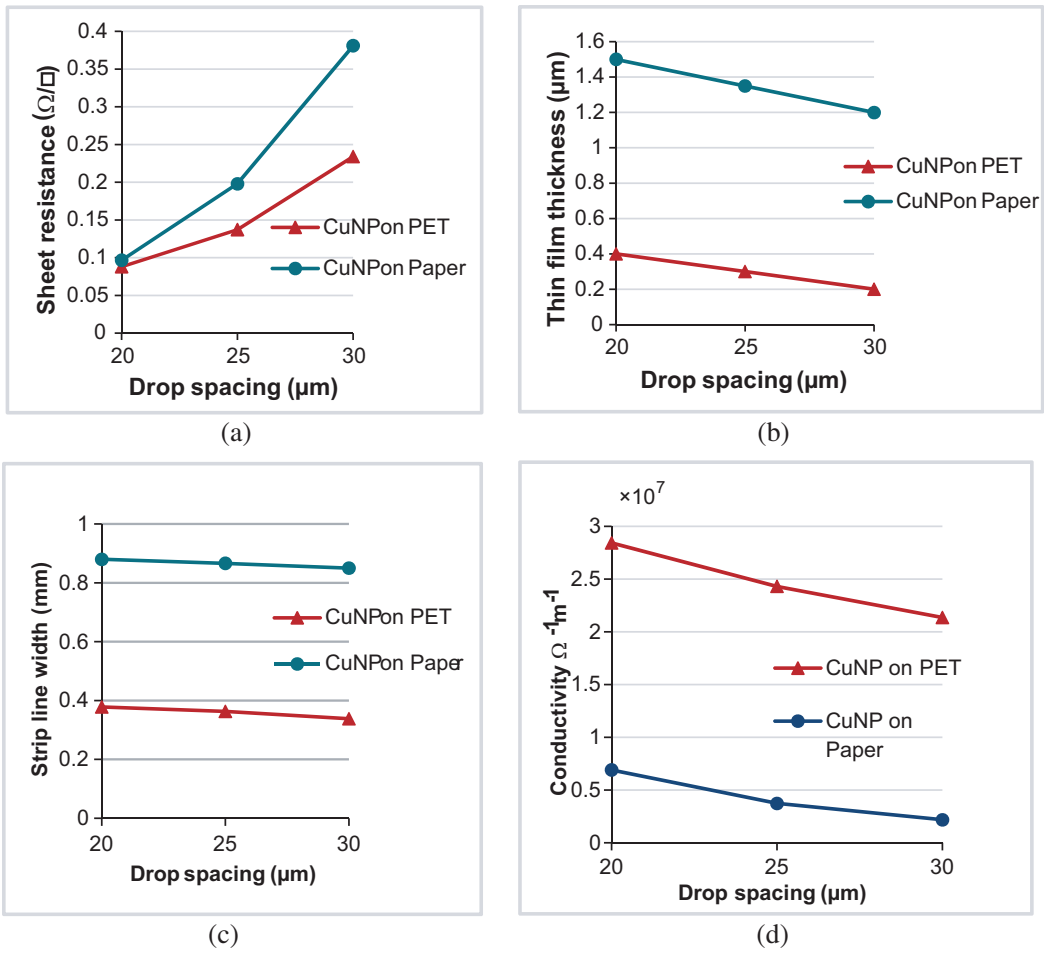

Figure 3. Drop spacing behavior for Copper nanoparticles on PET and Paper substrates against (a) sheet resistance, (b) thickness, (c) line width and (d) conductivity.

value for PET (−44 dB) than for paper substrate (−29 dB).

In order to validate our simulation results, the reflection coefficients $|S_{11}|$ of the fabricated antennas shown in Figs. 5(a) and 5(b) on both substrates were measured at the selected drop spacing of 20 µm using a Rohde & Schwarz ZVA67 Vector Network Analyzer.

The antennas are fed by solder-free 1.85 mm, 67 GHz model 1892-03A-6 Southwest Microwave female end launcher connector. The obtained values are plotted with the simulated ones as shown in Figs. 6(a) and 6(b) for the PET and paper substrates, respectively. The connector is included in the simulation model in CST-MWS to better simulate the measurement setup [27, 28]. The measured operating frequency has shifted to about 20.5 GHz. The discrepancies between the simulated and measured $|S_{11}|$ may be attributed to many reasons: the ground plane size of the CPW structure is way smaller than a quarter wavelength to practically excite correct even/odd modes, the capacitance loading, difficulty in precise alignment between the printed antenna and the fed-launcher and finally to fabrication tolerances. Table 3 shows the simulated antenna parameters for both substrates at different drop spacings.

By increasing the drop spacing, the gain, efficiency and bandwidth decrease while size reduction increases for both substrates. However, the difference in size reduction is totally negligible, and therefore the drop spacing of 20 µm shows the best performance as already noticed in the film conductivity (Section 3.1). We also notice that the performance of the antenna printed on PET is superior to the one printed on paper except for bandwidth. This is attributed to the fact that the film conductivity on PET is higher than on paper as shown in Fig. 3(d).

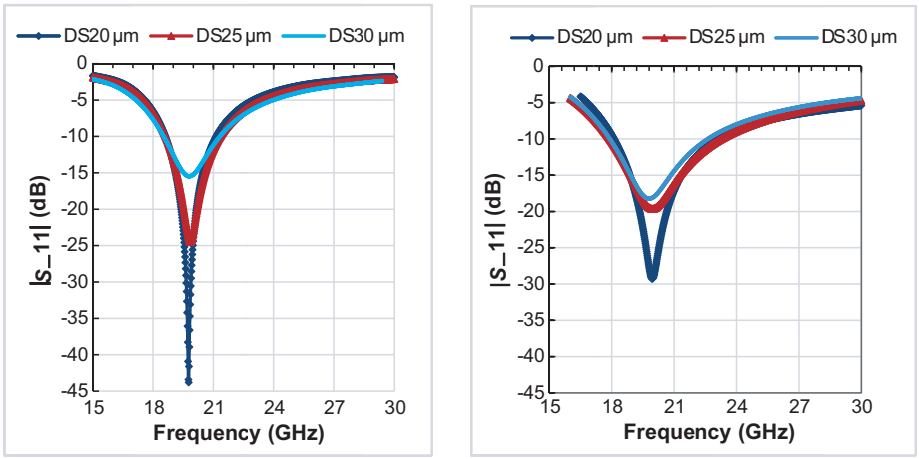

Figure 4. Comparison between the simulated reflection coefficient of CuONP on (a) PET substrate and (b) on paper substrate at different drop spacing 20 µm, 25 µm and 30 µm.

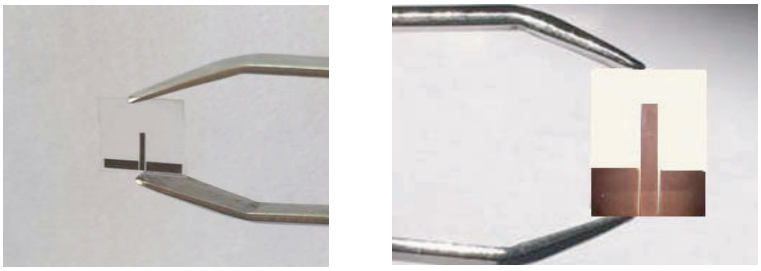

Figure 5. (a) Picture of the antenna printed on PET. (b) Picture of the antenna printed on paper.

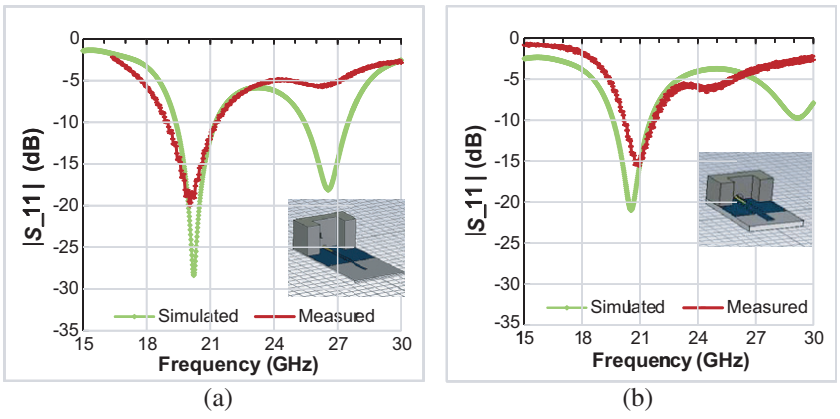

Figure 6. Comparison between the measured and simulated reflection coefficient of CuNP at drop spacing 20 µm. (a) PET substrate. (b) Paper substrate. The inset shows the end launcher.

3.3. Antenna Radiation Patterns

Table 4 shows the simulated radiation patterns taking into account the effects of the end launchers and the measured patterns for the antennas fabricated on both types of substrate at drop spacing of 20 µm. Better matching between the simulated and measured results is observed for the antennas printed on PET.

Table 3. Antenna parameters at different DSs for CuNp on PET and paper substrates.

	PET			Paper		
Drop spacing (µm)	20	25	30	20	25	30
Fractional BW $\mid -10$ dB %	13.92	13.58	12.67	26	24.23	23.2
Gain (dB)	1.82	1.73	1.71	1.41	1.1	0.98
Efficiency (%)	97.6	94.7	94.3	78.57	71.18	71.12
Size reduction (%)	98.87	99.2	99.4	95.8	96.23	96.66

Table 4. Simulated and measured radiation pattern of the CuNP-CPW monopole antenna at 20 GHz for PET and for paper dielectric substrates.

	PET	**Paper**
E-Plane [x-y]	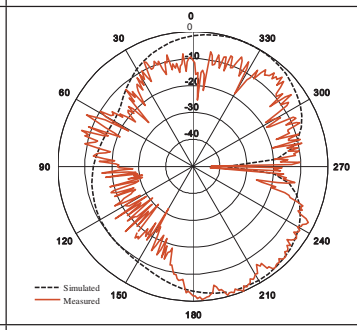	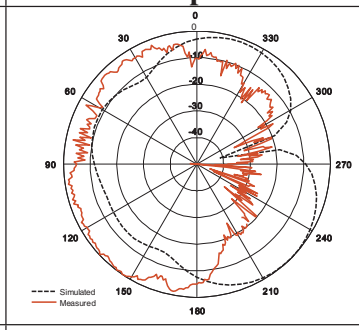
H-Plane [x-z]	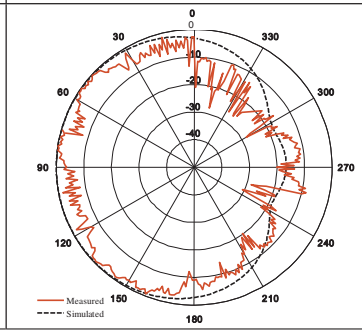	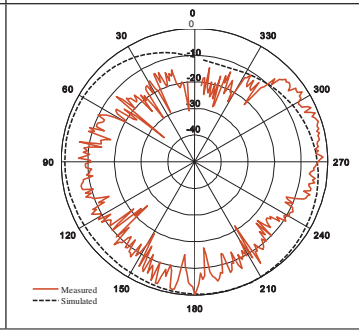

4. CONCLUSIONS

Low cost wideband coplanar waveguide-fed monopole antennas operating at 20 GHz were printed on PET and on paper substrates using copper oxide nanoparticles ink. The effect of varying the drop spacings was investigated experimentally and by numerical simulation. The adopted printing and curing techniques yielded a high conductivity of around $2.8 \times 10^7\,\Omega^{-1}\mathrm{m}^{-1}$, which is about 47% of the bulk material value. It was found that the best film conductivity and therefore antenna characteristics were obtained for the case of drop spacing 20 µm on PET substrate. Values less than 20 µm result in bulging of the printed lines while higher values cause a decrease in the film conductivity. The PET substrate showed a better performance because of the formation of thin copper films with regular grain structures due to its ability to uniformly spread the ink on its non-porous surface. On the other hand, thicker films on paper substrate are less uniform and exhibit a higher sheet resistance and therefore lower conductivity.

ACKNOWLEDGMENT

This work is a part of "SURSYS" project funded by German Academic Exchange Service (DAAD) and financed by the Federal Foreign Office of Germany. The authors are grateful for the support provided by Dr. Rami Ghannam of Cairo University, Kareem Elassy of the Arab Academy for Science, Technology and Maritime Transport, and Dr. Hans Marine Sauer of Technical University of Darmstadt.

REFERENCES

1. Çiftçi, T., B. Karaosmanoglu, and Ö. Ergül, "Low-cost inkjet antennas for RFID applications," *2015 Radio and Antenna Days of the Indian Ocean (RADIO), Belle Mare*, 1–2, Belle Mare, Mauritius, 2015.
2. Kang, H., H. Park, Y. Park, M. Jung, B. C. Kim, G. Wallace, and G. Choa, "Fully roll-to-roll gravure printable wireless (13.56 MHz) sensors-signage tags for smart packaging," *Scientific Reports*, Vol. 4, No. 5387, 2014.
3. Wegener, M., D. Spiehl, H. M. Sauer, F. Mikschl, X. Liu, N. Kölpin, M. Schmidt, M. P. M. Jank, E. Dörsam, and A. Roosen, "Flexographic printing of nanoparticulate tin-doped indium oxide inks on PET foils and glass substrates," *Journal of Materials Science*, Vol. 51, No. 9, 4588–4600, 2016.
4. Willmann, J., D. Stocker, and E. Dörsam, "Characteristics and evaluation criteria of substrate-based manufacturing. Is roll-to-roll the best solution for printed electronics?," *Organic Electronics*, Vol. 17, No. 7, 1631–1640, 2014.
5. Yousef, S. and A. Mohamed, "Mass production of CNTs using CVD multi-quartz tubes," *Journal of Mechanical Science and Technology*, Vol. 30, No. 11, 5135–5141, 2016.
6. Komoda, N., M. Nogi, K. Suganuma, K. Kohno, Y. Akiyama, and K. Otsuka, "Printed silver nanowire antennas with low signal loss at high-frequency radio," *Nanoscale*, Vol. 4, 3148–3153, 2012.
7. J. D. Lu, P. J. Deng, L. H. Li, and W. W. Li, "The research on gravure printing RFID antenna," *Advanced Materials Research*, Vol. 1033–1034, 1142–1148, 2014.
8. Bornemann, N., H. M. Sauer, and E. Dorsam, "Gravure printed ultrathin layers of small-molecule semiconductors on glass," *Journal of Imaging Science and Technology*, Vol. 55, No. 4, 2011.
9. Jan Špůrek, J. Vélim, M. Cupal, Z. Raida, J. Prášek, and J. Hubálek, "Slot loop antennas printed on 3D textile substrate," *21st International Conference on Microwave, Radar and Wireless Communications (MIKON)*, Gdansk, Poland, May 9–11, 2016.
10. Dokić, M., V. Radonić, A. Pleteršek, U. Kavčič, V. Crnojević-Bengin, and T. Muck, "Comparison between the characteristics of screen and flexographic printing for RFID applications," *Journal of Microelectronics, Electronic Components and Materials*, Vol. 45, No. 1, 3–11, 2015.
11. Kim, S., M. M. Tentzeris, and S. Nikolaou, "Wearable biomonitoring monopole antennas using inkjet printed electromagnetic band gap structures," *6th European Conference on Antennas and Propagation (EUCAP)*, Prague, Czech Republic, Mar. 26–Mar. 30, 2012.
12. Hassan, A., S. Ali, J. Bae, and C. H. Lee, "All printed antenna based on silver nanoparticles for 1.8 GHz applications," *Applied Physics A*, Vol. 122, 768, 2016.
13. Khonsari, Z., T. Björninen, M. M. Tentzeris, L. Sydänheimo, and L. Ukkonen, "2.4 GHz inkjet-printed RF energy harvester on bulk cardboard substrate," *IEEE Radio and Wireless Symposium (RWS)*, San Diego, CA, USA, Jan. 25–Jan. 28, 2015.
14. Roushdy, M. M. and H. F. Hammad, "Inkjet printed wearable Hilbert monopole fractal antenna optimized for BAN systems," *33rd National Radio Science Conference (NRSC)*, Aswan, Egypt, 2016.
15. http://www.fujifilmusa.com/press/news/display_news?newsID=880813.
16. Soltman, D. and V. Subramanian, "Inkjet-printed line morphologies and temperature control of the coffee ring effect," *Langmuir*, Vol. 24, No. 5, 2224–2231, 2008.

17. Poozesh, S., K. Saito, N. K. Akafuah, and J. Graña-Otero, "Comprehensive examination of a new mechanism to produce small droplets in drop-on-demand inkjet technology," *Applied Physics A*, Vol. 122, No. 110, 2016.
18. Albrecht, A., A. Rivadeneyra, A. Abdellah, P. Luglia, and J. F. Salmeróna, "Inkjet printing and photonic sintering of silver and copper oxide nanoparticles for ultra-low-cost conductive patterns," *Journal of Materials Chemistry C*, Vol. 4, 3546–3554, 2016.
19. Sipilä, E., J. Virkki, J. Wang, L. Sydänheimo, and L. Ukkonen, "Brush-painting and photonic sintering of copper oxide and silver inks on wood and cardboard substrates to form antennas for UHF RFID tags," *International Journal of Antennas and Propagation*, Vol. 2016, 2016.
20. Ten Brink, G. H., N. Foley, D. Zwaan, B. J. Kooia, and G. Palasantzas, "Roughness controlled superhydrophobicity on single nanometer length scale with metal nanoparticles," *RSC Advances*, Vol. 5, 28696–28702, 2015.
21. Van Der Pauw, L. J., "A method of measuring specific resistivity and hall effect of discs of arbitrary shape," *Philips Research Reports*, Vol. 13, 1–9, Feb. 1958.
22. Kang, J. S., H. S. Kim, J. Ryu, H. T. Hahn, S. Jang, and J. W. Joung, "Inkjet printed electronics using copper nanoparticle ink," *Journal of Materials Science: Materials in Electronics*, Vol. 21, No. 11, 1213–1220, 2010.
23. Zenou, M., O. Ermak, A. Saar, and Z. Kotler, "Laser sintering of copper nanoparticles," *Journal of Physics D: Applied Physics*, Vol. 47, No. 2, 2013.
24. Chena, C. N., C. P. Chena, T.-Y. Donga, T. C. Changb, M. C. Chenb, H. T. Chenc, and I. G. Chen, "Using nanoparticles as direct-injection printing ink to fabricate conductive silver features on a transparent flexible PET substrate at room temperature," *Acta Materialia*, Vol. 60, No. 16, 5914–5924, 2012.
25. Ahmed, S., F. A. Tahir, A. Shamim, and H. M. Cheema, "A compact Kapton-based inkjet-printed multiband antenna for flexible wireless devices," *IEEE Antennas and Wireless Propagation Letters*, Vol. 14, 1802–1805, 2015.
26. Wei, Y., Y. Li, R. Torah, and J. Tudor, "Laser curing of screen and inkjet printed conductors on flexible substrates," *Symposium on Design, Test, Integration and Packaging of MEMS/MOEMS (DTIP)*, Montpellier, France, Apr. 27–30, 2015.
27. Elsheakh, D. M. and M. F. Iskander, "Circularly polarized triband printed Quasi-Yagi antenna for millimeter-wave applications," *International Journal of Antennas and Propagation*, Vol. 2015, 2015.
28. Mehdipour, A., I. D. Rosca, A.-R. Sebak, C. W. Trueman, and S. V. Hoa, "Carbon nanotube composite for wideband millimeter-wave antenna applications," *IEEE Transactions on Antennas and Propagation*, Vol. 59, No. 10, 3572–3578, 2011.